Gene Therapy (2014) **21**, 514–521

www.nature.com/gt

ORIGINAL ARTICLE

Intranasal administration of plasmid DNA nanoparticles yields successful transfection and expression of a reporter protein in rat brain

BT Harmon[1], AE Aly[1], L Padegimas[2], O Sesenoglu-Laird[2], MJ Cooper[2] and BL Waszczak[1]

Viral vectors are a commonly used method for gene therapy because of their highly efficient transduction of cells. However, many vectors have a small genetic capacity, and their potential for immunogenicity can limit their usefulness. Moreover, for disorders of the central nervous system (CNS), the need for invasive surgical delivery of viruses to the brain also detracts from their clinical applicability. Here, we show that intranasal delivery of unimolecularly compacted DNA nanoparticles (DNA NPs), which consist of single molecules of plasmid DNA encoding enhanced green fluorescent protein (eGFP) compacted with 10 kDa polyethylene glycol (PEG)-substituted lysine 30-mers (CK30PEG10k), successfully transfect cells in the rat brain. Direct eGFP fluorescence microscopy, eGFP-immunohistochemistry (IHC) and eGFP-ELISA all demonstrated eGFP protein expression 2 days after intranasal delivery. eGFP-positive cells were found throughout the rostral-caudal axis of the brain, most often adjacent to capillary endothelial cells. This localization provides evidence for distribution of the nasally administered DNA NPs via perivascular flow. These results are the first report that intranasal delivery of DNA NPs can bypass the blood–brain barrier and transfect and express the encoded protein in the rat brain, affording a non-invasive approach for gene therapy of CNS disorders.

Gene Therapy (2014) **21**, 514–521; doi:10.1038/gt.2014.28; published online 27 March 2014

INTRODUCTION

Gene therapy for central nervous system (CNS) disorders includes investigation of viral vectors modified to transduce and over-express proteins with a known neuroprotective function. Viruses can inherently overcome barriers in order to deliver their genetic material to the nucleus, due to a variety of mechanisms that are hard to replicate in manufactured vectors.[1] However, several factors can limit the usefulness of viral vectors for this purpose, including their small genetic capacity, the possibility of host immune responses and inflammation, and the risk of oncogenicity arising from random insertion into genomic DNA.[2] In addition, the need for brain surgery to infuse a CNS gene therapy vector limits the clinical applicability of this approach. Therefore, two major areas of interest for CNS gene therapy are developing effective and non-inflammatory non-viral vectors, and dosing them in a non-invasive manner.

Copernicus Therapeutics Inc. has developed compacted DNA NPs comprising single molecules of DNA compacted with polycations and that have the minimum possible volume based on the partial specific volumes of DNA and the polycation.[3] The small size of these DNA NPs allows access via the nuclear membrane pore[3] and transfection of several types of non-dividing, post-mitotic cells.[3–6] A preferred polycation is a PEGylated lysine 30-mer (CK30PEG10k), which is highly active in transfecting proximal pulmonary epithelium after airway delivery,[5] the brain after direct brain injection,[6] and the retina after subretinal or intravitreal delivery.[4] These DNA NPs can be compacted into different shapes based, in part, on the lysine counterion at the time of DNA mixing.[7] Rod-shaped NPs, formulated with a CK30PEG10k polycation having an acetate counterion, have minimal cross-sectional diameters of 8–11 nm, which is independent of the plasmid size. Long-term lung, brain and retina expression has been demonstrated after a single injection.[8–13] These CK30PEG10k DNA NPs have been shown to be non-immunogenic and non-inflammatory,[6,14,15] and encouraging results were noted in an initial DNA NP clinical trial in cystic fibrosis subjects,[16] with no adverse events due to the NPs and positive functional assays in dosed subjects.

Intranasal delivery offers a novel means by which larger molecular weight therapeutics can gain direct access to the brain. The mechanisms by which intranasally delivered substances enter the CNS have not been fully elucidated, but it is thought to involve a combination of perineuronal, perivascular and lymphatic transport pathways, largely dependent on the region where the delivered agent is placed within the nasal cavity and the physicochemical properties of the therapeutic being administered.[17] Transport from the nasal epithelium appears to follow the olfactory and trigeminal nerve pathways, resulting in delivery to the olfactory bulbs as well as to more caudal brain areas, respectively. Within the brain, pulsatile flow in perivascular spaces has been postulated to allow for widespread transport of molecules within interstitial fluid to sites deep in the parenchyma.[18–21] For a recent in-depth report on the mechanisms of intranasal delivery to the brain, see the review by Lochhead and Thorne.[22] Numerous groups have successfully used the intranasal route to deliver proteins,[20,23–25] siRNA,[26,27] miRNA,[28] viral vectors[29–34] and even stem cells[35,36] to the brain. However, successful intranasal delivery to the brain of a non-viral vector for gene therapy has not yet been demonstrated.

[1]Department of Pharmaceutical Sciences, Northeastern University, Boston, MA, USA and [2]Copernicus Therapeutics, Inc., Cleveland, OH, USA. Correspondence: Dr BL Waszczak, Pharmaceutical Sciences, Northeastern University, Room 269, 140 The Fenway, 360 Huntington Avenue, Boston, MA 02115, USA.
E-mail: b.waszczak@neu.edu
Received 26 August 2013; revised 12 February 2014; accepted 17 February 2014; published online 27 March 2014

The focus of the current study is to determine whether intranasal administration could deliver a non-viral gene vector to the brain, resulting in successful transfection and protein expression. We have thus utilized unimolecularly compacted DNA NPs encompassing enhanced green fluorescent protein (eGFP) transcriptionally controlled by the CMV promoter, referred to as pCG. Fluorescence microscopy of eGFP, eGFP-IHC and eGFP-ELISA were performed to qualitatively and quantitatively determine eGFP production after intranasal administration of pCG DNA NPs. Our results show widespread eGFP brain expression, indicating that intranasal delivery of this non-viral vector bypasses the blood–brain barrier and is a feasible approach for CNS gene therapy. Moreover, localization of eGFP-positive cells near capillary endothelial cells provides evidence for perivascular flow as a potential mechanism of transport and distribution of the DNA NPs within the brain.

RESULTS

Supplementary Figure 1 shows the plasmid map of the 3.6 kb eGFP expression plasmid, pCG. Expression is driven by the cytomegalovirus (CMV) promoter and the CMV transcriptional enhancer region, which allows for highly efficient and ubiquitous protein production in mammalian cells. However, as CMV promoters are prone to rapid silencing, especially in brain,[6,37] we chose a 2-day post-delivery time point to observe maximum protein expression.

Striatal injection of CK30PEG10k pCG nanoparticles successfully transfects brain cells

Initial experiments were conducted to confirm that the pCG NPs were capable of successful transfection and eGFP expression in the rat brain after a direct injection of the construct into the brain parenchyma. A dose of 4 µl (3.9 mg ml^{-1} DNA) pCG NPs was injected stereotaxically into the left striatum, and rats were killed 2 days post injection. eGFP expression was visualized using eGFP-IHC and by fluorescence microscopy (Figures 1a–c).

Examination of striatal sections revealed heavy, local expression of eGFP confined to the area directly surrounding the needle track. eGFP-IHC was a more sensitive means of detection, insofar as a larger number of eGFP-positive cells and a wider area of transfection adjacent to the needle track were apparent by IHC compared with direct fluorescence. Cells expressing eGFP were densely clustered and overlapping, making it difficult to assess cellular morphology, that is, whether they were neurons, glia or vascular elements. This study confirmed that CK30PEG10 DNA NPs were capable of transfecting cells in the rat brain when injected directly into the striatum.

Intranasal CK30PEG10kpCG nanoparticles express eGFP in the rat brain

To assess whether intranasal administration of pCG NPs could transfect cells in the brain and lead to protein expression, rats were given an intranasal dose of 25 µl of pCG NP (3.9 mg ml^{-1}), naked pCG plasmid (3.9 mg ml^{-1}) or intranasal saline, and killed 2 days later. Levels of eGFP expression were analyzed in ~2 mm thick coronal sections spanning the rostral-to-caudal axis of the brain. Each coronal section was further divided into dorsal and ventral areas, and the 13 regions were assayed by eGFP-ELISA.

Overall, there was a higher level of eGFP expression in the brains of animals administered intranasal pCG NPs relative to those given the naked plasmid or saline (Figure 2; one-way analysis of variance (ANOVA), $P = 0.0002$; Tukey's post test for pCG NP vs saline, $P < 0.001$, and for pCG NP vs naked pCG, $P < 0.01$). The levels of expression varied considerably by brain area, and in the naked pCG-treated rats eGFP levels were close to the limit of detection of the assay in some regions, that is, baseline levels in the saline-treated controls. Because of this variability, only the hindbrain (D) showed significant differences in eGFP expression due to treatment (one-way ANOVA, $P < 0.05$; Tukey's post test pCG NP vs saline, $P < 0.05$). However, collectively, these results demonstrate that the pCG NPs were able to reach and transfect cells in areas spanning the rostral-caudal axis of the rat brain following intranasal administration.

To determine whether transfection and eGFP expression could be detected in the brain by fluorescence microscopy and eGFP-IHC, another set of rats was administered the same intranasal treatments, and the rats were killed 2 days later by transcardial perfusion with 4% paraformaldehyde. Coronal sections taken from the entire rostral-caudal axis of brain were examined for qualitative evidence of transfection. Sparse but widespread cellular expression was observed throughout the brains of rats given intranasal pCG NPs by direct fluorescent microscopy. Representative images from the midbrain and striatum are shown in Figures 3c and d. However, only cells with large amounts of eGFP expression were detectable above background autofluorescence. The sparse distribution of these green fluorescent cells may therefore underestimate the actual number of cells that were successfully transfected and produced eGFP. In addition, intranasal administration of the naked pCG plasmid also caused a very sparse transfection of cells in each brain area (Figure 3b). In all cases, the cells producing eGFP were often found along the edges of capillaries, suggesting they might be associated with the vascular endothelium (Figures 3b–d).

Some sections from each of the treated rats were also subjected to eGFP-IHC, as IHC may allow for more sensitive detection.

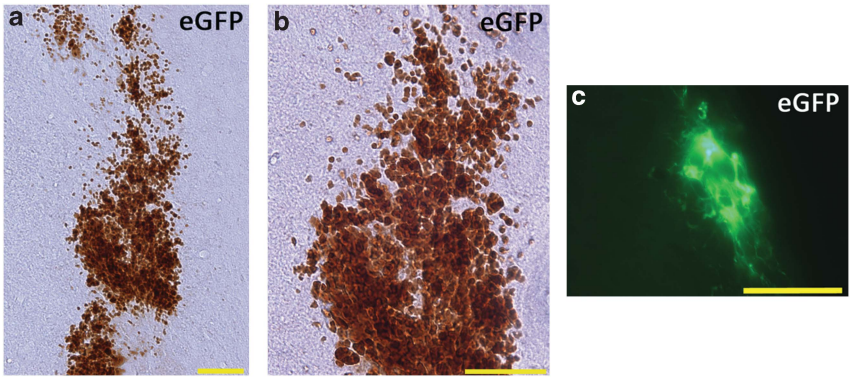

Figure 1. Detection of eGFP in rat corpus striatum 2 days after pCG DNA NP injection. eGFP expression was detected by IHC and by direct fluorescence microscopy 2 days after injection of CK30PEG10k pCG NPs (15.6 µg) in rat striatum. (**a**, **b**) Immunostaining at the injection track (×20 and ×40, respectively). (**c**) eGFP fluorescence along needle track (×40). Scale bars = 50 µm.

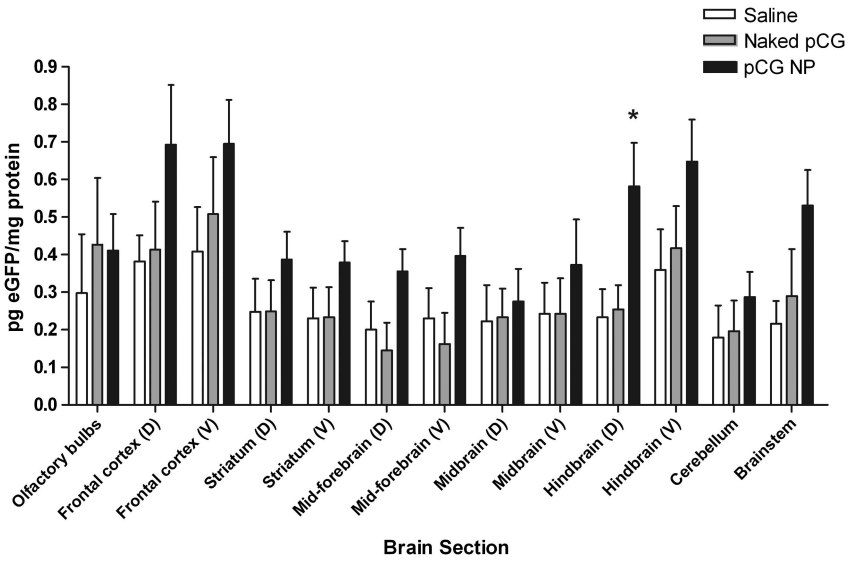

Figure 2. eGFP-ELISA of rat brain sections 2 days after intranasal administration of pCG nanoparticles or naked DNA. Rats were dosed intranasally with 97.5 μg of pCG NPs or naked pCG (25 μl, both at a DNA concentration of 3.9 mg ml^{-1}), or saline. Two days later, brains were sectioned and eGFP levels were assayed by ELISA. Values were normalized to mg protein for each section. Bars represent the mean eGFP expression (pg eGFP/mg protein+s.e.m.). Overall, eGFP expression was significantly higher in the brains of rats given intranasal pCG NPs ($n = 6$) than in those given intranasal naked pCG ($n = 5$) or saline ($n = 5$). Significance of treatments was determined by one-way ANOVA ($P = 0.0002$), and Tukey's post test showed significant differences for pCG NP vs saline ($P < 0.001$) and pCG NP vs naked pCG ($P < 0.01$). Within individual brain regions, a significant effect was observed only in the hindbrain (one-way ANOVA, $P < 0.05$; Tukey's post test, pCG NP vs saline, $P < 0.05$). D, dorsal; V, ventral.

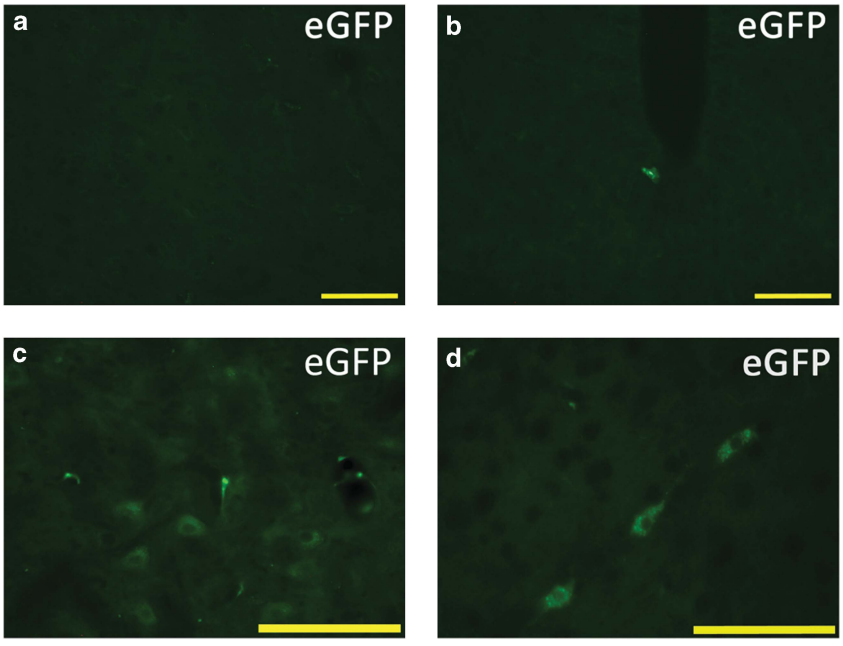

Figure 3. Native eGFP expression in the rat brain as observed by fluorescence microscopy 2 days after intranasal administration of pCG or saline. (**a**) No discrete cellular fluorescence was seen in sections from rats given intranasal saline. (**b**) Fluorescent cells were observed rarely in sections from rats given intranasal naked pCG plasmid. (**c**, **d**) A sparse but widespread distribution of fluorescent cells was observed in sections from rats given intranasal pCG NPs. Fluorescent cells were typically adjacent to capillaries. (**a**) striatum (×20); (**b**) midbrain (×20); (**c**) midbrain (×40); (**d**) striatum (×40). Scale bars = 50 μm.

Expression patterns detected by IHC were similar to those of that observed by direct fluorescence, although larger numbers of immunostained cells were found. Moreover, rats given intranasal pCG NPs showed higher numbers of cells than rats given intranasal naked pCG or saline. This difference is illustrated in representative images from the midbrain of rats from each treatment group (Figure 4). Similar differences were observed in the other brain areas. Cells expressing eGFP often appeared clustered together and, like those seen by direct fluorescence microscopy, seemed to align along capillaries.

To further quantify eGFP expression in the brains of the treated rats, eGFP-immunostained cells were counted in one representative section from each of six brain regions (A through F) of each rat in each intranasal treatment group (Figure 5). The total number of

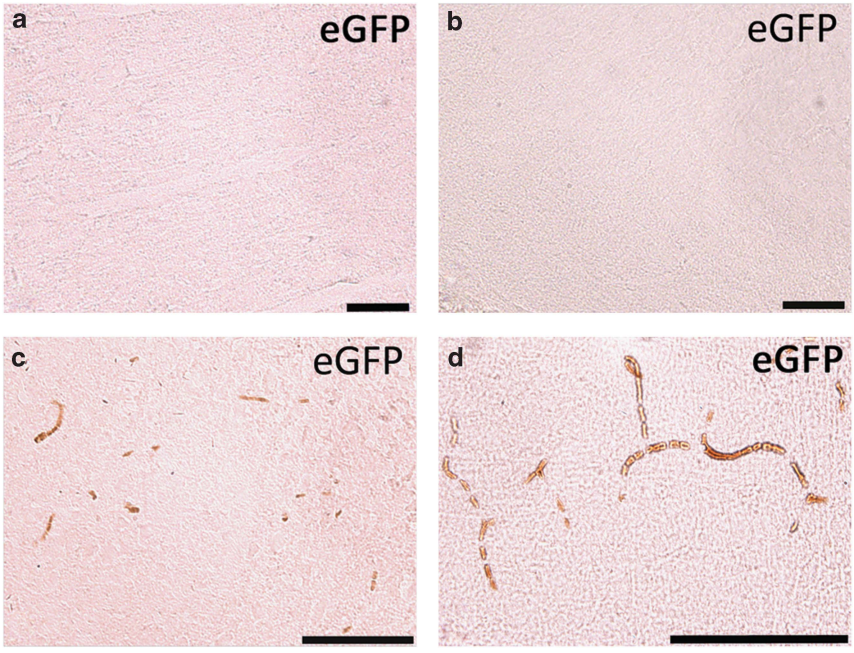

Figure 4. eGFP-IHC in the rat brain 2 days after intranasal administration of pCG or saline. Sections from saline-treated (**a**) and naked pCG-treated (**b**) rats showed a lack of cellular immunostaining for eGFP. Sections from rats given intranasal pCG NPs (**c**, **d**) showed plentiful eGFP-positive cells, which appeared to align along capillaries. All are representative sections taken from the midbrain. (**a**, **b**) ×20; (**c**) ×40; (**d**) ×80 optical zoom. Scale bars = 50 μm.

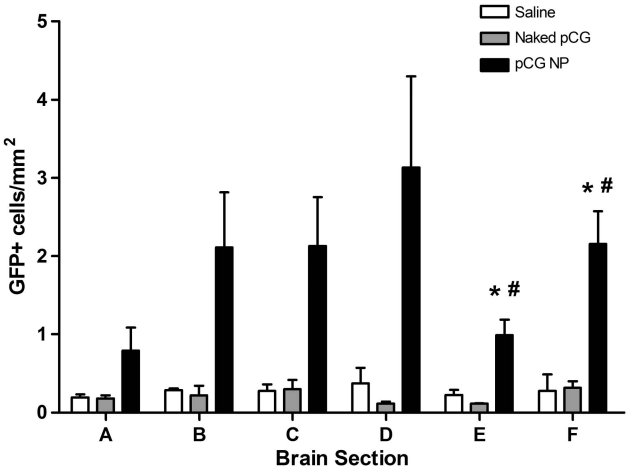

Figure 5. Quantification of eGFP-immunolabeled cells from rats 2 days after intranasal pCG NPs, naked pCG or saline. One representative section from each coronal brain region (A through F) was observed at ×20 per rat. Bars represent the mean eGFP-positive cell count normalized to section area (mm^2)+s.e.m. for pCG NP ($n = 5$), naked pCG-($n = 3$) or saline ($n = 3$)-treated rats. Labeled cells in saline controls represent non-specific staining. eGFP-labeled cells were consistently and significantly greater in rats treated with pCG NPs than naked pCG or saline. One-way ANOVA showed an overall significant effect by treatment ($P < 0.0001$), and Tukey's post test showed significance for pCG NPs vs saline ($P < 0.001$) and pCG NPs vs naked pCG ($P < 0.001$). Within individual brain areas, one-way ANOVA showed significant differences in sections E and F ($P < 0.01$ and $P < 0.05$, respectively). Tukey's post test indicated significance for pCG NP vs saline ($^{*}P < 0.05$) and pCG NP vs naked pCG ($^{\#}P < 0.05$). Brain sections: A is frontal cortex; B is forebrain; C is diencephalon; D is midbrain; E is hindbrain; F is cerebellum/brainstem.

eGFP-positive cells was quantified for each region, normalized to section area and averaged for each of the treated rats (Figure 5 and Supplementary Table 1). Overall, the number of eGFP-positive cells, as well as the number of cells per mm^2, was significantly higher in the brains of rats administered pCG NPs than those given intranasal naked pCG or saline treatments (one-way ANOVA, $P < 0.0001$; Tukey's post test for pCG NP vs saline, $P < 0.001$, and for pCG NP vs naked pCG, $P < 0.001$). When data for the individual regions were analyzed, significant differences between treatment groups were found in sections E and F, the most caudal brain areas (one-way ANOVA, $P < 0.01$ and $P < 0.05$, respectively; Tukey's post test for pCG NP vs saline, $P < 0.05$, and for pCG NP vs naked pCG, $P < 0.05$, in both areas). Again, these results confirm that intranasal administration of pCG NPs achieves transfection and expression of eGFP along the rostral-caudal axis of the rat brain.

Intranasal pCG leads to transfection of perivascular cells

To further examine the cell type(s) transfected following intranasal administration of pCG NPs, sections from regions A, C and D of one of the treated rats were subjected to double-label IHC for eGFP and rat endothelial cell antigen-1 (RECA-1). As in the previous study, eGFP-positive cells, which appeared red due to labeling with an Alexa Fluor 647-conjugated secondary antibody, were detected throughout each of the regions analyzed. Of a total of 144 eGFP-positive cells from section A (frontal cortex), 161 cells from section C (forebrain at the level of the anterior commissure) and 106 cells from section D (midbrain), 81.9, 87.0, and 81.6%, respectively, were immediately adjacent to and overlapping RECA-1 staining of capillary endothelial cells, which appeared green due to a secondary antibody conjugated to Alexa Fluor 488. The remaining eGFP-positive cells were adjacent to endothelial cells but not directly overlapping. In all cases, however, the eGFP-positive cells appeared to align along the capillary endothelium, abluminal to and in close juxtaposition to the endothelial cell membrane. Figure 6 shows images of eGFP-positive cells from each of the brain areas examined, along with their coregistration with RECA-1-postive cells. This perivascular localization suggests that the transfected cells are part of the neurovascular unit, and most likely pericytes.

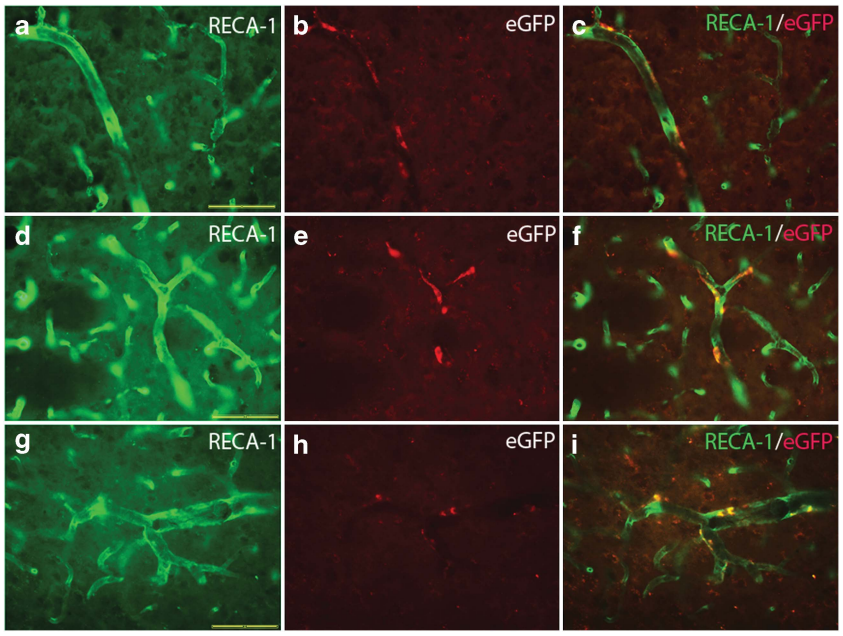

Figure 6. RECA-1 and eGFP double-label immunohistochemistry in the rat brain 2 days after intranasal delivery of pCG nanoparticles. (**a**–**c**) Frontal cortex section stained for RECA-1 and eGFP. (**d**–**f**) A striatum section stained for RECA-1 and eGFP. (**g**–**i**) A midbrain section stained for RECA-1 and eGFP. Left panels show RECA-1 labeling (green). Middle panels show eGFP labeling of the same field (red). Right panels show merged images for each series. All images were captured at ×40. Scale bars = 40 μm.

DISCUSSION

For non-viral gene therapy to ultimately succeed clinically in treating disorders of the brain, the vector would have to be capable of transfecting cells that allow expression of the protein of interest in the target regions affected by the disease process. To provide proof-of-principle, we used a plasmid (pCG) encoding the enhanced green fluorescent protein gene transcriptionally controlled by the CMV promoter. Direct injection of pCG NPs into the rat striatum resulted in a clear and discrete expression of eGFP in cells along the needle track 2 days after injection. eGFP was visible both by direct fluorescence and by eGFP-IHC, although the latter means of detection was more sensitive in revealing transfected cells. This preliminary study confirmed the ability of the compacted pCG NPs to achieve transfection in the brain.

Most importantly, nasal delivery of pCG NPs produced widespread transfection and expression of eGFP throughout the brain. The NP preparation was superior to the naked pCG plasmid insofar as it generated significantly higher eGFP expression, both as detected by ELISA and by counts of eGFP-positive cells along the rostral-caudal axis of the brain. Overall, eGFP expression was observed from the most rostral sections of brain (that is, the frontal cortex) to the most caudal sections (encompassing the hindbrain, cerebellum and brainstem). Protein levels were the highest in the frontal cortex, hindbrain and brainstem, whereas cell counts were higher in all regions of the pCG NP-treated rats than in controls, with significant increases in the hindbrain and brainstem. The olfactory bulbs, which receive axonal inputs from the olfactory nerve, were not examined by fluorescence microscopy or eGFP-IHC, but somewhat surprisingly did not exhibit increases in protein expression above control levels. This may indicate that the olfactory nerve was not the main conduit for nose-to-brain transport of the NPs in this study. Nevertheless, the rostral-caudal pattern of expression, with relatively higher levels in frontal cortex and hindbrain/brainstem, does suggest that entry into the brain was mediated by extracellular transport of the NPs along nerve tracks of the olfactory and trigeminal nerves. These nerve tracks extend from the nasal cavity to rostral brain areas, such as the frontal cortex, as well as caudal areas, such as the brainstem and spinal cord, respectively. Thorne *et al.*[20,25,38] have shown that proteins administered by the nasal route travel along the olfactory and trigeminal nerves to achieve their highest levels in the forebrain and brainstem, respectively. Our results are in good agreement with this pattern of distribution.

When eGFP-immunostained cells were counted and normalized to section area, the number of stained cells was significantly higher across rostral-caudal areas of brain in the pCG NP treatment group compared with the naked pCG- and saline-treated groups. This result was in general agreement with the ELISA data. However, the magnitude of the differences in the number of eGFP-positive cells between the pCG NP-treated rats and controls greatly exceeded the differences observed by ELISA. Moreover, the distribution of labeled cells did not closely match the expression pattern seen with ELISA. For instance, mean eGFP cell counts in the pCG NP-treated rats tended to be higher even in areas such as midbrain where eGFP expression levels were only marginally above control levels. These differences bring to light not only inherent limitations of the assays for detecting low-level transfection and expression but also the low efficiency of the nasal route of administration. For other intranasally administered substances, such as proteins, the amount transported to the brain has been shown to be a fraction of a percentage of the administered dose.[23,25,38] By extrapolation, if a similar fraction of the nasally administered DNA NPs reached the brain, expression would be expected to be low. Nevertheless, even low-level expression, such as that observed here, could represent bioactive protein levels within the therapeutic range for a number of CNS disorders, provided the protein reached its intended target(s) in the brain. Many neurotrophic factors, which have high potencies at their target cells, fall into this category.

As a first step toward identifying the cell types in the brain that become transfected after intranasal delivery, microscopic analyses revealed that the eGFP-positive cells were found along capillaries and aligned in clusters. In a previous study, intranasal delivery to mice of a naked plasmid encoding β-galactosidase was reported to result in detection of plasmid DNA in microvessel endothelial

cells in the brain, although transfection of these cells was not explicitly demonstrated.[39] In our study, transfection of perivascular cells was confirmed by IHC, and the labeled cells were found much more commonly in rats that received pCG NPs than the naked plasmid. This result underscores the critical importance of the CK30PEG10k NP formulation in achieving transfection.

Considering the hypothetical mechanism of distribution of intranasally administered substances by perivascular flow,[20,25] the cells most likely to first interact with the NPs as they travel through interstitial fluid in the brain might be those lining perivascular spaces, that is, cells lying just outside the capillary endothelium, at the interface between the vascular compartment and the surrounding parenchyma. Pulsatile flow within these perivascular spaces[18,19,21] has been postulated as the transport mechanism by which nasally administered substances spread throughout the brain.[20,25] The fact that eGFP-positive cells virtually always lie adjacent to RECA-1 staining of capillaries identifies them as components of the neurovascular unit and provides evidence for distribution of the NPs by the perivascular transport system. Alternatively, transfection of perivascular cells could theoretically occur by transport of the NPs via the systemic circulation. This would require vascular absorption in the nasal cavity, circulation to the brain and subsequent transcytosis of the NPs across vascular endothelial cells once in the brain. Such a mechanism has been postulated as a potential means of delivery of NPs to the brain after nasal administration.[40,41] This possibility cannot be ruled out, as we did not examine brain transfection after intravenous administration of pCG NPs. However, it is unlikely insofar as we have shown that nasal administration of CK30PEG DNA NPs does not yield detectable expression of the transgene in other highly vascularized tissues, such as the liver or the heart, as would be expected if the NPs gained access to the systemic circulation.[5]

The cells comprising the neurovascular unit include the major constituents of the blood–brain barrier, namely endothelial cells, pericytes and astrocyte endfeet. As the eGFP-labeled cells were located adjacent and abluminal to the endothelial cells, it is tempting to speculate that they may be pericytes, which typically surround and envelope the endothelial cells.[42,43] Brain pericytes have an important role in maintaining integrity of the blood–brain barrier by their production and release of soluble factors that regulate endothelial cell tight junctions and microvessel permeability.[42,44,45] Indeed, pericytes are now regarded as a novel therapeutic target for neurological disorders.[46] If the transfected cells are mainly pericytes, this suggests several potential advantages and limitations of intranasal delivery of CK30PEG10k DNA NPs for CNS disorders. As pericyte coverage of the microvasculature is extremely high in the brain, transfection of even a small percentage of these cells by nasally administered DNA NPs could lead to widespread protein expression in the brain. If diffuse production and release of a therapeutic protein were desirable for a particular brain disorder, or at least not detrimental, it could be an advantage having pericytes serving as the primary source of protein production. This might be the case for clinical conditions where the gene therapy was intended to augment expression of an endogenous neurotrophic factor at multiple targets sites in the brain. Any effects of the expressed protein would presumably be limited to cells expressing surface receptors for the trophic factor, but, even so, off-target effects in unintended brain areas would need to be examined. Moreover, production of such protein ligand molecules might have enhanced brain parenchymal distribution based on perivascular flow dynamics. On the other hand, if the gene therapy was intended to transfect a specific neural or glial cell population to correct an underlying intracellular defect, the predominance of perivascular celltransfection would limit this approach for such clinical indications. Further *in situ* double-labeling studies will be required to better understand the percentage and regional distribution of transfected perivascular cells compared with neurons and glial cells. In addition, only a single dosing regimen has been evaluated, and DNA NP dose and a variety of intranasal delivery parameters may influence brain transfection efficiency as well as the cell types transfected. Hence, dosing optimization studies will be of key importance when considering potential clinical development of intranasal DNA NPs.

Another consideration is whether the protein detected by ELISA in particular brain areas might represent transport from other sites. It is possible that transfection and protein expression may occur at any locus within the intranasal pathway, from the nasal epithelium to the olfactory and trigeminal nerves, to the cells encountered as the NPs traverse the brain and CSF. Although eGFP-IHC provides qualitative evidence that cells lining perivascular spaces in the brain express eGFP, the protein also may be transported from the cells that expressed it. For instance, cells lining the olfactory or trigeminal nerves, which might be preferentially transfected, could serve as a depot for expression of protein and lead to a similar distribution throughout the brain. It is known that improperly folded eGFP can be secreted through non-classical pathways in mammalian cells,[47] so this mechanism could contribute to the detection of eGFP even in areas where cellular transfection and protein expression were limited.

In summary, these studies demonstrate that intranasal delivery of CK30PEG10k DNA NPs can lead to the expression of a protein of interest in the rat brain. To our knowledge, this is the first report that intranasal administration of a non-viral DNA NP vector can lead to brain transgene expression. These results further show that the cells transfected within the brain are likely to be pericytes, which may have certain advantages for delivery of candidate therapeutics intended to act at receptors on neurons and/or glial cells. In addition, our finding that perivascular cells were transfected by DNA NPs lends support to the hypothesis that distribution of nasally administered substances occurs via perivascular transport. These findings provide proof-of-principle that this non-viral DNA NP vector administered by the intranasal route can achieve transfection and expression of the encoded gene in the brain, thereby affording a non-invasive means of gene therapy for CNS disorders. While the single dose and time point selected in this study yielded modest transgene expression, increased levels of expression may be attainable using higher doses of DNA or multiple dosing strategies. Further optimization of the dose, dosing regimen and dose interval will be important to achieve appropriate levels of transgene expression. The non-invasive nature of intranasal delivery of DNA NPs as a means of introducing and expressing a therapeutic gene in the brain has clinical merit, and the potential therapeutic benefits certainly warrant the effort for optimization of this approach.

MATERIALS AND METHODS

Formulation of compacted DNA nanoparticles

Twenty milliliters of pCG DNA solution (0.1 mg ml^{-1}) was slowly added to a mixing solution of 2.0 ml (3.2 mg ml^{-1}) of CK30PEG10k (American Peptide Company, Sunnyvale, CA, USA) having an acetate counterion.[5,7] Compacted DNA was filtered through a sterile 0.2-μm polyethersulfone membrane and then processed with tangential flow filtration in exchange with saline. Further concentration steps were performed using VIVASPIN centrifugal concentrators (MWCO 100k). The final concentration of pDNA used in both compacted and naked pCG treatments was 3.9 μg μl^{-1}.

Treatments

Male Sprague–Dawley (SD) rats weighing 225–250 *g* (Taconic, Germantown, NY, USA) were used in accordance with an approved Northeastern University IACUC protocol. For intranasal delivery, rats were anesthetized with ketamine and xylazine (90/20 mg kg^{-1}, i.p.) and placed in the supine position with their noses upright and their heads flat on the surface. Rats were given solutions of either naked plasmid (3.9 mg ml^{-1}), compacted

plasmid nanoparticles (3.9 mg ml^{-1}) or saline via a Hamilton syringe fitted with a short piece of polyethylene tubing. Intranasal doses were given in 2.5 µl increments every minute alternating nares for a total of 25 µl (97.5 µg pCG). Rats remained supine for 30 min post treatment.

For intracerebral injections, rats were anesthetized with ketamine and xylazine (90/20 mg kg^{-1}kg, i.p.) and placed in a stereotaxic apparatus. A total of 4 µl (15.6 µg) of pCG was surgically injected into the left striatum at the following stereotaxic coordinates: +2.5 mm lateral to lambda, +0.7 mm anterior to bregma, −5.8 mm ventral to the surface of the skull. The solution was injected at a rate of 1 µl min^{-1}. The needle was left at the injection site for 10 min to ensure that the solution fully dispersed before it was slowly removed. The entire stereotaxic surgery was done under aseptic technique, and skin was closed using tissue glue. Rats were given an injection of buprenorphine (0.05 mg kg^{-1}, s.c.) before recovery from anesthesia to minimize post-surgical pain.

eGFP-ELISA

Two days after intranasal administration, rats (5–6/group) were anesthetized with isoflurane and killed by decapitation. Their brains were rapidly removed and ~2 mm thick coronal sections were cut using a Plexiglas brain matrix. The fresh brain sections were flash frozen on dry ice (CO_2) before being stored at −80 °C. Before the ELISA, each section was homogenized in 1 ml of lysis buffer (1% Igepal, 10% glycerol and 1:100 protease inhibitor in PBS) and centrifuged at 4 °C for 30 min at 14 000 r.p.m. The resulting supernatant was used as the sample for the ELISA.

A96-well Nunc-immunoplate was used for the assay, and the total volume of all solutions was maintained at 100 µl per well. Plates were incubated at room temperature with continuous shaking. The wells were first coated with the capture antibody diluted 1:4000 in PBS (mouse anti-GFP #G-6539, Sigma, St Louis, MI, USA) and incubated overnight at 4 °C. After this and each subsequent step, the plate was washed three times with wash buffer (0.05% Tween-20 in PBS) and blotted dry using paper towels. Blocking buffer (5% non-fat dry milk in PBS) was then added at room temperature for 1 h. Reagent diluent (1% BSA in PBS) was used for blanks and subsequent dilutions. Samples and blanks were then added, and the plate was incubated at room temperature for 2 h. Next, detection antibody (rabbit anti-GFP conjugated to HRP #NB100–1184, Novus Biologicals, Littleton, CO, USA) diluted 1:2000 in reagent diluent was added, and the plates were incubated for another 2 h. For color development, SureBlue TMB substrate (KPL, Gaithersburg, MD, USA) was added, and the plate was incubated for 10–20 min. The reaction was stopped with 1N HCl. Optical density was read at 450 and 570 nm using a BioTek ELx800 microplate reader (Biotek, Winooski, VT, USA) and Gen5 software. To express eGFP in terms of mg protein present in the samples, a BCA protein assay (Pierce BCA Protein Assay Kit #23227, Thermo Scientific, Waltham, MA, USA) was run concurrent with each ELISA in accordance with the manufacturer's protocol.

Immunohistochemistry

Two days after intranasal administration, rats (3–5/group) were killed by transcardial perfusion with 4% paraformaldehyde (PF). Brains were post-fixed overnight in 4% PF and then submerged in 30% sucrose for 48–72 h. Brains were cut into ~2 mm thick coronal sections using a Plexiglas rat brain matrix, and each was cryostat-cut to yield 30 µm sections spanning the rostral-caudal axis of the brain. The sections were stored at 4 °C in cryoprotectant until the day of assay. For single-label eGFP-IHC, the sections were first washed three times with PBS (10 min each) and then treated with 0.3% H_2O_2 for 15 min to inhibit endogenous peroxidases. Subsequent wash steps between incubations took place using a PBS-Triton Buffer containing 0.1% Triton-X 100 (three times for 10 min each). Tissue was then blocked with 10% normal donkey serum (NDS) in PBS for 30 min at room temperature to decrease non-specific binding. For chromogenic detection of eGFP, brain sections were incubated for 2 h at room temperature on a rotating wheel with the primary antibody (rabbit anti-GFP conjugated to HRP #NB100-1184, Novus Biologicals) diluted 1:2000 in PBS-Triton buffer. 3-3′-Diaminobenzidine (DAB) (Vector Labs, Burlingame, CA, USA) was prepared according to kit instructions and incubated with the sections for 12 min to visualize the peroxidase-catalyzed reaction product.

For double-label immunofluorescence detection of eGFP and RECA-1, brain sections were washed as described previously and blocked using a solution containing 10% NDS and 10% normal goat serum (NGS) in PBS for 1 h. Sections were then incubated overnight at 4 °C on a rotating wheel with both primary antibodies (rabbit anti-GFP #ab290, Abcam, Cambridge, MA, USA and mouse anti-RECA-1 #ab9774, Abcam) diluted 1:2000 and 1:1000 in PBS containing 5% NDS and 5% NGS, respectively. The following day, sections were incubated at room temperature for 2 h with the corresponding secondary antibodies (donkey anti-rabbit IgG conjugated to Alexa Fluor 647 #ab150075, Abcam and goat anti-mouse IgG conjugated to Alexa Fluor 488 #ab150117, Abcam), each diluted 1:2000 in PBS.

Microscopy

All microscopic analyses were performed using an Olympus BX51 with X-cite fluorescence and DIC optics for contrast enhancement. Sections were mounted on slides using Fluoromount-G (Southern Biotech, Birmingham, AL, USA). Bright field microscopy was used to detect the chromogenic signal from DAB for single-label eGFP-IHC. The number of DAB-positive cells was counted manually at ×20 magnification in one representative section from each of the six regions for each brain. Counting was performed by an observer blinded to the treatments. Fluorescence microscopy using a FITC excitation/emission filter set was used to observe native eGFP. Fluorescence microscopy for detection of RECA-1 (Alexa-488) and eGFP (Alexa-647) double labeling was performed using excitation/emission filter sets for both red and green. Bioquant Nova version 6.90.1 image analysis software was used for counting of eGFP-positive cells in the single-labeling study and for conducting conditional frequency analyses of eGFP-positive cells that were in register with RECA-1 in the double-labeling study. The conditional frequency analysis of double labeling was done for 2–14 sections from each of three brain regions of a rat given intranasal pCG nanoparticles. Results were expressed as the percentage of eGFP positive cells that coregistered with RECA-1-positive cells.

Statistical analysis

One-way analysis of variance (ANOVA) and appropriate *post hoc* tests to determine significant differences between treatment groups were performed using GraphPad Prism software, version 4.03. The α-level for significance was set at $P < 0.05$. Data are presented as mean ± s.e.m. Outliers were eliminated on the basis of the Grubb's test (GraphPad Prism) or in instances where values were less than the blank value+3 s.d. in the eGFP-ELISA.

CONFLICT OF INTEREST

LP, OSL and MJC are employed by Copernicus Therapeutics.

ACKNOWLEDGEMENTS

We gratefully acknowledge the assistance of Dr Justin Manjourides, biostatistician in the Department of Health Sciences at Northeastern University, for advice on methods of statistical analysis and interpretation. We also thank Amanda Nadeau for technical assistance in counting eGFP-positive cells. Brendan Harmon was supported by an IGERT Nanomedicine Science & Technology Award NSF-DGE-0965843 to Northeastern University. Funding for this research was provided in part by a Northeastern University 2011-2012 Provost's Tier 1 Interdisciplinary Grant and by the Michael J. Fox Foundation for Parkinson's Research.

REFERENCES

1 Thomas CE, Ehrhardt A, Kay MA. Progress and problems with the use of viral vectors for gene therapy. *Nat Rev Genet* 2003; **4**: 346–358.
2 Lentz TB, Gray SJ, Samulski RJ. Viral vectors for gene delivery to the central nervous system. *Neurobiol Dis* 2012; **48**: 179–188.
3 Liu G, Li D, Pasumarthy MK, Kowalczyk TH, Gedeon CR, Hyatt SL *et al.* Nanoparticles of compacted DNA transfect postmitotic cells. *J Biol Chem* 2003; **278**: 32578–32586.
4 Farjo R, Skaggs J, Quiambao AB, Cooper MJ, Naash MI. Efficient non-viral ocular gene transfer with compacted DNA nanoparticles. *PLoS One* 2006; **1**: e38.
5 Ziady AG, Gedeon CR, Miller T, Quan W, Payne JM, Hyatt SL *et al.* Transfection of airway epithelium by stable PEGylated poly-L-lysine DNA nanoparticles *in vivo*. *Mol Ther* 2003; **8**: 936–947.
6 Yurek DM, Fletcher AM, Smith GM, Seroogy KB, Ziady AG, Molter J *et al.* Long-term transgene expression in the central nervous system using DNA nanoparticles. *Mol Ther* 2009; **17**: 641–650.

7 Fink TL, Klepcyk PJ, Oette SM, Gedeon CR, Hyatt SL, Kowalczyk TH *et al.* Plasmid size up to 20 kbp does not limit effective *in vivo* lung gene transfer using compacted DNA nanoparticles. *Gene Therapy* 2006; **13**: 1048–1051.
8 Fletcher AM, Kowalczyk TH, Padegimas L, Cooper MJ, Yurek DM. Transgene expression in the striatum following intracerebral injections of DNA nanoparticles encoding for human glial cell line-derived neurotrophic factor. *Neuroscience* 2011; **194**: 220–226.
9 Han Z, Conley SM, Makkia R, Guo J, Cooper MJ, Naash MI. Comparative analysis of DNA nanoparticles and AAVs for ocular gene delivery. *PLoS One* 2012; **7**: e52189.
10 Padegimas L, Kowalczyk TH, Adams S, Gedeon CR, Oette SM, Dines K *et al.* Optimization of hCFTR lung expression in mice using DNA nanoparticles. *Mol Ther* 2012; **20**: 63–72.
11 Yurek DM, Fletcher AM, McShane M, Kowalczyk TH, Padegimas L, Weatherspoon MR *et al.* DNA nanoparticles: detection of long-term transgene activity in brain using bioluminescence imaging. *Mol Imaging* 2011; **10**: 327–339.
12 Cai X, Conley SM, Nash Z, Fliesler SJ, Cooper MJ, Naash MI. Gene delivery to mitotic and postmitotic photoreceptors via compacted DNA nanoparticles results in improved phenotype in a mouse model of retinitis pigmentosa. *FASEB J* 2010; **24**: 1178–1191.
13 Han Z, Conley SM, Makkia RS, Cooper MJ, Naash MI. DNA nanoparticle-mediated ABCA4 delivery rescues Stargardt dystrophy in mice. *J Clin Invest* 2012; **122**: 3221–3226.
14 Ziady AG, Gedeon CR, Muhammad O, Stillwell V, Oette SM, Fink TL *et al.* Minimal toxicity of stabilized compacted DNA nanoparticles in the murine lung. *Mol Ther* 2003; **8**: 948–956.
15 Ding XQ, Quiambao AB, Fitzgerald JB, Cooper MJ, Conley SM, Naash MI. Ocular delivery of compacted DNA-nanoparticles does not elicit toxicity in the mouse retina. *PLoS One* 2009; **4**: e7410.
16 Konstan MW, Davis PB, Wagener JS, Hilliard KA, Stern RC, Milgram LJ *et al.* Compacted DNA nanoparticles administered to the nasal mucosa of cystic fibrosis subjects are safe and demonstrate partial to complete cystic fibrosis transmembrane regulator reconstitution. *Hum Gene Ther* 2004; **15**: 1255–1269.
17 Dhuria SV, Hanson LR, Frey 2nd WH. Intranasal delivery to the central nervous system: mechanisms and experimental considerations. *J Pharm Sci* 2010; **99**: 1654–1673.
18 Wang P, Olbricht WL. Fluid mechanics in the perivascular space. *J Theor Biol* 2011; **274**: 52–57.
19 Hadaczek P, Yamashita Y, Mirek H, Tamas L, Bohn MC, Noble C *et al.* The "perivascular pump" driven by arterial pulsation is a powerful mechanism for the distribution of therapeutic molecules within the brain. *Mol Ther* 2006; **14**: 69–78.
20 Thorne RG, Pronk GJ, Padmanabhan V, Frey 2nd WH. Delivery of insulin-like growth factor-I to the rat brain and spinal cord along olfactory and trigeminal pathways following intranasal administration. *Neuroscience* 2004; **127**: 481–496.
21 Rennels ML, Blaumanis OR, Grady PA. Rapid solute transport throughout the brain via paravascular fluid pathways. *Adv Neurol* 1990; **52**: 431–439.
22 Lochhead JJ, Thorne RG. Intranasal delivery of biologics to the central nervous system. *Adv Drug Deliv Rev* 2012; **64**: 614–628.
23 Migliore MM, Vyas TK, Campbell RB, Amiji MM, Waszczak BL. Brain delivery of proteins by the intranasal route of administration: a comparison of cationic liposomes versus aqueous solution formulations. *J Pharm Sci* 2010; **99**: 1745–1761.
24 Liu XF, Fawcett JR, Thorne RG, DeFor TA, Frey 2nd WH. Intranasal administration of insulin-like growth factor-I bypasses the blood-brain barrier and protects against focal cerebral ischemic damage. *J Neurol Sci* 2001; **187**: 91–97.
25 Thorne RG, Hanson LR, Ross TM, Tung D, Frey 2nd WH. Delivery of interferon-beta to the monkey nervous system following intranasal administration. *Neuroscience* 2008; **152**: 785–797.
26 Kim ID, Shin JH, Kim SW, Choi S, Ahn J, Han PL *et al.* Intranasal delivery of HMGB1 siRNA confers target gene knockdown and robust neuroprotection in the postischemic brain. *Mol Ther* 2012; **20**: 829–839.
27 Renner DB, Frey 2nd WH, Hanson LR. Intranasal delivery of siRNA to the olfactory bulbs of mice via the olfactory nerve pathway. *Neurosci Lett* 2012; **513**: 193–197.
28 Lee ST, Chu K, Jung KH, Kim JH, Huh JY, Yoon H *et al.* miR-206 regulates brain-derived neurotrophic factor in Alzheimer disease model. *Ann Neurol* 2012; **72**: 269–277.
29 Lemiale F, Kong WP, Akyurek LM, Ling X, Huang Y, Chakrabarti BK *et al.* Enhanced mucosal immunoglobulin A response of intranasal adenoviral vector human immunodeficiency virus vaccine and localization in the central nervous system. *J Virol* 2003; **77**: 10078–10087.
30 Zhang J, Wu X, Qin C, Qi J, Ma S, Zhang H *et al.* A novel recombinant adeno-associated virus vaccine reduces behavioral impairment and beta-amyloid plaques in a mouse model of Alzheimer's disease. *Neurobiol Dis* 2003; **14**: 365–379.
31 Laing JM, Gober MD, Golembewski EK, Thompson SM, Gyure KA, Yarowsky PJ *et al.* Intranasal administration of the growth-compromised HSV-2 vector DeltaRR prevents kainate-induced seizures and neuronal loss in rats and mice. *Mol Ther* 2006; **13**: 870–881.
32 Draghia R, Caillaud C, Manicom R, Pavirani A, Kahn A, Poenaru L. Gene delivery into the central nervous system by nasal instillation in rats. *Gene Therapy* 1995; **2**: 418–423.
33 Jiang Y, Wei N, Zhu J, Zhai D, Wu L, Chen M *et al.* A new approach with less damage: intranasal delivery of tetracycline-inducible replication-defective herpes simplex virus type-1 vector to brain. *Neuroscience* 2012; **201**: 96–104.
34 Damjanovic D, Zhang X, Mu J, Medina MF, Xing Z. Organ distribution of transgene expression following intranasal mucosal delivery of recombinant replication-defective adenovirus gene transfer vector. *Genet Vaccines Ther* 2008; **6**: 5.
35 Danielyan L, Schafer R, von Ameln-Mayerhofer A, Buadze M, Geisler J, Klopfer T *et al.* Intranasal delivery of cells to the brain. *Eur J Cell Biol* 2009; **88**: 315–324.
36 Reitz M, Demestre M, Sedlacik J, Meissner H, Fiehler J, Kim SU *et al.* Intranasal delivery of neural stem/progenitor cells: a noninvasive passage to target intracerebral glioma. *Stem Cells Transl Med* 2012; **1**: 866–873.
37 Gray SJ, Foti SB, Schwartz JW, Bachaboina L, Taylor-Blake B, Coleman J *et al.* Optimizing promoters for recombinant adeno-associated virus-mediated gene expression in the peripheral and central nervous system using self-complementary vectors. *Hum Gene Ther* 2011; **22**: 1143–1153.
38 Thorne RG, Frey 2nd WH. Delivery of neurotrophic factors to the central nervous system: pharmacokinetic considerations. *Clin Pharmacokinet* 2001; **40**: 907–946.
39 Han IK, Kim MY, Byun HM, Hwang TS, Kim JM, Hwang KW *et al.* Enhanced brain targeting efficiency of intranasally administered plasmid DNA: an alternative route for brain gene therapy. *J Mol Med* 2007; **85**: 75–83.
40 Patel T, Zhou J, Piepmeier JM, Saltzman WM. Polymeric nanoparticles for drug delivery to the central nervous system. *Adv Drug Deliv Rev* 2012; **64**: 701–705.
41 Wong HL, Wu XY, Bendayan R. Nanotechnological advances for the delivery of CNS therapeutics. *Adv Drug Deliv Rev* 2012; **64**: 686–700.
42 Sa-Pereira I, Brites D, Brito MA. Neurovascular unit: a focus on pericytes. *Mol Neurobiol* 2012; **45**: 327–347.
43 Dore-Duffy P. Pericytes: pluripotent cells of the blood brain barrier. *Curr Pharm Des* 2008; **14**: 1581–1593.
44 Shimizu F, Sano Y, Abe MA, Maeda T, Ohtsuki S, Terasaki T *et al.* Peripheral nerve pericytes modify the blood-nerve barrier function and tight junctional molecules through the secretion of various soluble factors. *J Cell Physiol* 2011; **226**: 255–266.
45 Shimizu F, Sano Y, Saito K, Abe MA, Maeda T, Haruki H *et al.* Pericyte-derived glial cell line-derived neurotrophic factor increase the expression of claudin-5 in the blood-brain barrier and the blood-nerve barrier. *Neurochem Res* 2012; **37**: 401–409.
46 Lange S, Trost A, Tempfer H, Bauer HC, Bauer H, Rohde E *et al.* Brain pericyte plasticity as a potential drug target in CNS repair. *Drug Discov Today* 2013; **18**: 456–463.
47 Tanudji M, Hevi S, Chuck SL. Improperly folded green fluorescent protein is secreted via a non-classical pathway. *J Cell Sci* 2002; **115**(Pt 19): 3849–3857.

Supplementary Information accompanies this paper on Gene Therapy website (http://www.nature.com/gt)